MULTIDISCIPLINARY SCIENCE JOURNAL

RESEARCH ARTICLE
Published Online: XXXX xx, 2025
https://doi.org/10.31893/multiscience.2025609

A study of meteorological drought via the SPI and SPEI with special reference to groundwater depth in the drought prone area of west bengal

Sutrisha Ghosh[a] | **Nayan Roy**[a] | **Rolee Kanchan**[a]

[a]Department of Geography, Faculty of Science, The Maharaja Sayajirao University of Baroda, Vadodara, India.

Abstract Drought is a worldwide phenomenon that affects almost all geographical regions, causing enormous harm to both the natural environment and human life. Drought frequency and intensity vary according to natural and anthropogenic factors. It has a significant impact on agriculture, hydrology, economics, ecology and human societies. Recognizing the implications for drought preparation, mitigation, and action. Moreover, identifying and mitigating drought vulnerability is essential for decision makers. Meteorological drought analysis provides a thorough examination of all meteorological factors, such as precipitation, wind speed, relative humidity, dew point, vapor pressure and evaporation. The standardized precipitation index (SPI) and standardized precipitation evapotranspiration index (SPEI) at different timescales were used for 1998--2018 to analyze the drought characteristics. According to SPI calculations, the months of January through July are experiencing extreme drought. According to the SPEI, the extremely dry months are from March to August and from October to December. The results of the Mann–Kendall (M-K) test and Sen's slope analysis revealed that the postmonsoon drought tendency increased more rapidly than did the other two periods. Holt-Winter's test calculates the trend with seasonal change. It was used to anticipate the weather for the following 10 years and indicated that the drought propensity would worsen in the next years. The groundwater level is an essential indicator of water availability for humans. In the tropics, groundwater levels respond to excessive precipitation. As drought can be observed during the postmonsoon season, the postmonsoonal water level depth tends to rise gradually.

Keywords: Drought, Groundwater level, Holt–Winter test, Mann–Kendall test, Sen's slope, SPEI, SPI

1. Introduction

Droughts are slow-onset events induced by climate change and with acute shortages of water. It is one of the most pervasive climatic risks, with no universal description; it is not a well-defined criterion for evaluating its intensity; and it has no definite starting point or end date. It is one of the most destructive natural catastrophes owing to its impact on agricultural activity and water supplies, and it has caused serious economic, environmental, and sociological difficulties throughout the world (Getahuhn and Li, 2023). This phenomenon plays a role in different segments of nature and can generally be defined as meteorological, hydrological and agricultural drought. Socioeconomic drought refers to the association of these three elements (Ding et al., 2021). The intensity varies depending on the duration and period of occurrence of the event. With respect to several drought occurrences, meteorological drought is more severe since its severity can lead to surface and subterranean water shortages, crop yield declines, losses in soil moisture and reductions in socioeconomic amenities. This can result in reduced water storage and affect the water supply in water conservancy projects, social economic water use and ecological water use (Tsakiris, 2017; Heim, 2002). Water scarcity destroys the agricultural water balance and reduces crop output, causing food issues and even hunger. Drought may also have an impact on ecosystem stability and can even kill animals during severe drought seasons owing to a lack of suitable drinking water (Ledger et al., 2011, Wang et al., 2019). The Irrigation Commission of India, Government of India (1976), denotes a scenario in which yearly rainfall is less than 75% of average rainfall (Parthasarathy et al., 1987; Shah et al., 2015). The prevalence of meteorological drought seems to be correlated with a shortage of monsoon rainfall, while rising temperatures could worsen drought. Drought conditions are very common in subhumid regions in India because of the irregular and uneven distribution of monsoons and the long range of extremely high temperatures (Pathak and Dodamani, 2019). Many studies have shown that subhumid regions of India are facing increasing trends in the severity of drought. Drought is considered a natural hazard, and in recent decades, it has had a significant influence on the global environment. Water scarcity disrupts the agricultural water balance and results in lower crop production or an unsuccessful harvest. It will also create food issues and even hunger. Drought may also affect ecosystem stability and potentially kill animals during severe drought seasons owing to a lack of sufficient drinking water (Ledger et al.

 Received: February 1, 2025 | Accepted: April 22, 2025

2011). Drought has had a substantial impact on all of these factors in recent years, especially in light of increasing population, agricultural expansion, and industrial and economic development (Ahmadalipour et al., 2019, Wang et al., 2019). Therefore, people need to pay particular attention to drought.

Various meteorological drought indices are important for monitoring dry and wet conditions at a single value on the basis of various parameters related to meteorological aspects. Indices such as the surface water supply index (SWSI) (Shafer and Dezman., 1982), rainfall anomaly index (Rooy, 1965), Palmar drought severity index (Palmar, 1965), crop moisture index (CMI) (Palmer, 1968), Bhalme and Mooley drought index (Bhalme and Mooley, 1980), standardized precipitation index (SPI) (Mckee, 1995), effective drought index (EDI) (Byun and Wilhite., 1999), reclamation drought index (RDI) (Tsakiris and Vangeli, 2005), and standardized precipitation evapotranspiration index are important for delineating meteorological drought. For agricultural drought, the moisture adequacy index (MAI) (McGuire and Palmer, 1957), crop moisture index (CMI) (Palmer, 1968), crop-specific drought index (Meyer et al., 1993), and soil moisture deficit and evapotranspiration deficit index (Narsimhan and Srinivas, 2005) are the major indices. Similarly, the surface water supply index (SWSI), standardized hydrological index (SHI), standardized water supply index (SWSI) (Shafer and Dezman, 1982), standardized runoff index (SRI) (Shukla and Wood, 2008), and standardized streamflow index (SSI) (Vicente-Serrano et al., 2012) are the major indices for hydrological drought.

To determine the intensity, duration and geographic extent of drought, the World Meteorological Organization recommends calculating the standardized precipitation index (SPI) and the standardized precipitation evapotranspiration index (SPEI) (Nedealcov et al., 2015). The SPI and SPEI have advantages, as these techniques employ previous cumulative climatic conditions, which also influence the value of the present index and are more valuable characteristics. The SPI is based on precipitation data, whereas the SPEI is based on precipitation and evaporation-transpiration data. These two drought indicators are extremely important for tracking the degree of precipitation, determining water levels, estimating agricultural production, monitoring the frequency of wildfires and other events (Shaik, 2020; NOAA.,2021).

Soil moisture decreases when associated with precipitation anomalies within a relatively short time frame. Groundwater, river flow and reservoir accumulation reflect long-term precipitation anomalies. To satisfy seasonal rainfall characteristics, McKee et al. estimated the SPI for several time intervals (3, 6, 12, 24 and 48 months) (Bhunia et al., 2020). The SPI is a basic index based on the chance of precipitation, and its calculation requires monthly precipitation data for at least 30 years. The precipitation is normalized via a probability distribution, and the SPI values are displayed as standard deviations from the median.

Table 1 Categorization of SPI and SPEI values.

Climatic moisture categories	SPI or SPEI
Extremely wet	≥2.0
Severely wet	1.5 to 1.99
Moderately wet	1.0 to 1.49
Normal	0.99 to - 0.99
Moderate drought	- 1.0 to - 1.49
Severe drought	- 1.5 to - 1.99
Extreme drought	≤- 2.0

Source: McKee (1995).

The SPEI relies on potential evapotranspiration, which calculates atmospheric precipitation, temperature and latitude, vapor pressure, solar radiation, and elevation of the area. It is an index-based computation process, and the drought categories are the same as the available SPI time scales. The SPEI calculation is based on the monthly difference between precipitation and potential evapotranspiration, which is a simple water balance approach. As a result, a comprehensive collection of atmospheric and water balance data is employed to calculate the same values (Nedealcov et al., 2015). The increasing pattern of evaporation caused by global warming is a significant component of drought analysis. In this context, the SPEI is superior to the SPI. However, compared with the SPI, the use of the SPEI in arid climates is severely limited. As an outcome, implementing a relative assessment of these indicators yields the best results on the basis of the area of concern. India is one of the most drought-prone countries in the world, with the most rainfall occurring during the southeast monsoon (June--September) and insufficient rainfall causing drought in various regions (Kumar et al., 2013).

Exponential smoothing is a relatively recent concept in this discipline and was created in the field of corporate mathematics in 1960 (Mishra and Desai, 2005). The exponential smoothing approach is a highly accurate scientific method for simulating and forecasting drought, particularly meteorological drought. A long-term drought tendency curve was generated via the exponential smoothing technique in Bankura (Raha and Gayen., 2019).

Li et al. (2020), Wang et al. (2019), Liu et al. (2020), Vicente-Serrano et al. (2015), etc., compared the SPEI with the SPI to identify drought incidence at the regional level across different climatic zones. Several studies (Roy et al., 2022; Zhai et al., 2020; Nath et al., 2017) have been conducted on drought analysis in India, and they reported increasing trends in drought severity and frequency over the agriculturally significant subhumid eastern region of the country in recent decades.

Shahfahad et al. (2023), Kundu et al. (2020), and Panday et al. (2020) used the SPI to examine the distribution and intensity of meteorological droughts in India. Several current studies suggest that the evapotranspiration-based SPEI is an improved indicator when it combines with the precipitation-based SPI for drought incidence in subhumid regions of India (Roy et al., 2023; Bera et al., 2021; Monish and Rehana, 2020; Li et al., 2020; Singh and Shukla, 2020; Singh et al., 2019; Pathak and Dodamani, 2019). Drought conditions are frequent in the subhumid regions of India because of the disproportionate distribution of monsoon rainfall with rising temperatures (Pandey and Srivastava, 2019). Additionally, every region has unique climatic features that interact differently with anthropogenic activities and climate change. In previous decades, the western part (Chotonagpur Plateau) of Purulia has been subjected to short-term droughts (Jha et al., 2013).

Groundwater level monitoring via well data is the primary source of information on the impact of hydrologic stresses on groundwater systems (Ahmadi and Sedghamiz, 2006). Groundwater storage fluctuations correspond well with interannual rainfall variability. In the humid area of Benin, recharge occurs periodically and linearly in response to rainfall reaching an apparent threshold of between 140 and 250 mm/year (Kotchoni et al., 2018). In this work, the trend of groundwater level fluctuations was analyzed to determine how far it changed according to drought and wet conditions.

This study aims to fill the research gap of actual recent scenarios of meteorological drought in the Chotonagpur Plateau in the west to plain valley in eastern Purulia district with justifications for the surface water scenario and water depth (borehole data). There is a significant absence of monsoonal rainfall scenarios and trends of irregular rainfall to understand the actual period of drought in this semiarid region for water stress management. The water demand is greater than the amount of water available in this region. Serious water scarcity and recurring drought incidents are occurring in this area. The main objective of this study is to determine the conditions, trends, intensities and drought forecasts via the SPI and SPEI for a specified period and determine the strong relationships between precipitation and evapotranspiration and the groundwater level.

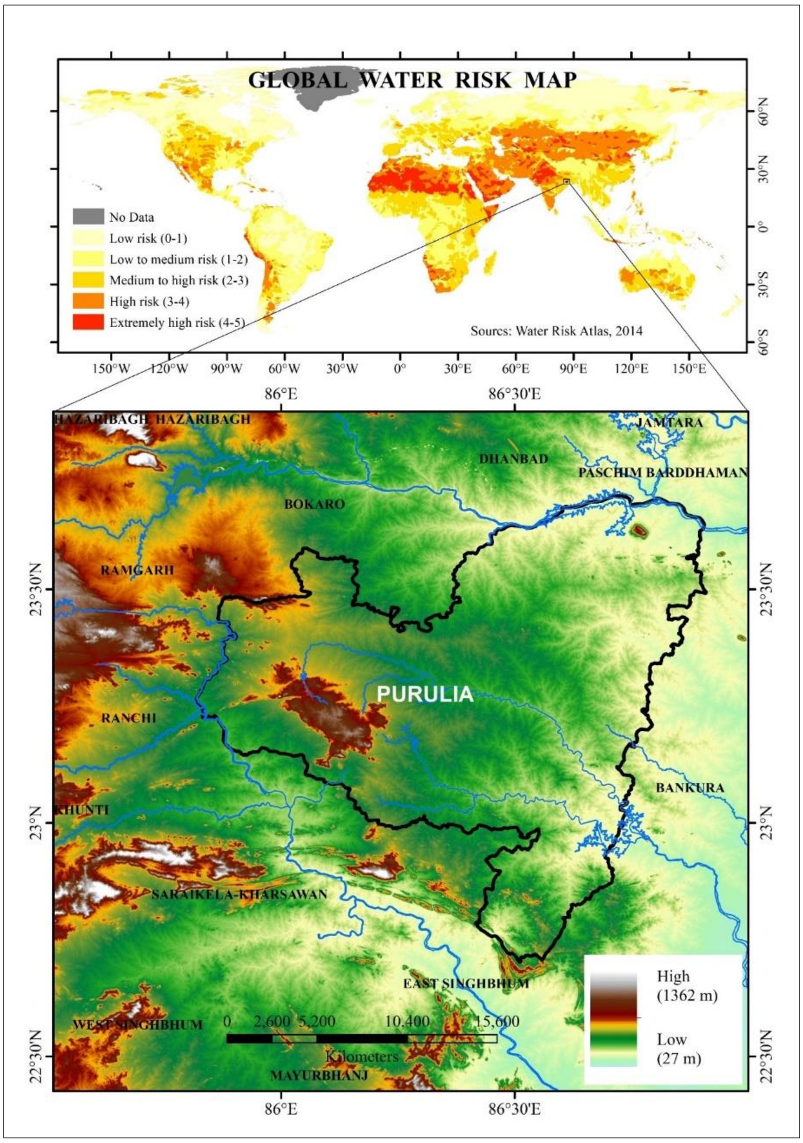

Figure 1 Study area.

2. Materials and Methodology

2.1. Study Area

The Purulia district, located in western West Bengal, is an eastern section of the Chota Nagpur Plateau. The research region lies between latitudes 22°42’35’’N to 23°42’’N and longitudes 85°49’25’’E to 86°54’37’’E. The district has a total size of 6259 km2 and 20 Community Development blocks. Purulia is well recognized as a drought-prone area and is located in the state's semiarid zone. The district is located in the agroclimatic area of the Eastern Plateau and Hills, as well as the subregions of the Chhotonagpur South and West Bengal Plateau. The climate in the district is subtropical, with significant evaporation and relatively little precipitation. The primary lithological formations of the studied region are mostly igneous and metamorphic rocks (i.e., granite and granitic gneiss), which sculpt a distinct physical environment and topographical differences throughout the district (CGWB, 2022). The annual rainfall ranges between 1100 and 1500 mm. During the monsoon season, the relative humidity ranges from 75% to 80%. In the scorching summer, however, it decreases to 25% to 35%. Temperatures range from 7°C in the winter to 46.8°C in the summer (District Disaster Management Plan, 2020--2021).

2.2. Dataset

In this study, rainfall and temperature data from the previous 21 years (1998--2018) in the Purulia district were used to calculate the standardized precipitation index (SPI) and standardized precipitation evapotranspiration index (SPEI). Monthly data on precipitation, maximum minimum temperature, wind speed, radiance, etc., attributes were gathered from the NASA website (https://giovanni.gsfc.nasa.gov/giovanni/). Drought indices (SPI, SPEI) can be developed with a minimum of 20-year datasets. The SPI was computed for Hunan Province for 20 years (1989--2008), where the climate is a monsoon humid type of subtropical weather (Zhang et al., 2019). The groundwater level data from 1998--2018 were downloaded from the Central Groundwater Board.

2.3. Standardized Precipitation Index (SPI)

A long-term monthly rainfall series is required for the SPI computation (McKee et al., 1993, Getahun and Li, 2023) for a specified time scale and location. This index was designed to recognize the scarcity of rainfall and the severity of drought. The probability density function (PDF) of an appropriate distribution is derived to characterize the long-term time series of observed precipitation. The cumulative probability of observed precipitation is calculated. The SPI is then calculated by applying the inverse normal (Gaussian) function to the cumulative probability, with a mean of zero and a variance of one (Pathak & Dodamani., 2019). The rainfall data (1998--2018) were fitted to a gamma distribution function in this case.

The R programming language has been utilized to study the SPI values. The formula is used to calculate the Gamma distribution's likelihood function.

$$g(x) = \frac{1}{\beta \propto \Gamma(\alpha)} x^{\alpha-1} e^{-x/\beta} \qquad (1)$$

where α= shape, β=scale and x= amount of precipitation.

The standardized precipitation index (SPI) uses the same rule as the Z score, as written below:

$$SPI = \frac{X-\mu}{\sigma} \qquad (2)$$

where X= actual precipitation, μ= average precipitation and σ= standard deviation of the dataset.

2.4. Standardized Precipitation Evapotranspiration Index (SPEI)

Vicente-Serrano et al. developed the SPEI (Vicente-Serrano et al., 2010). The SPEI considers both rainfall and temperature components and depicts the impact of evaporation deviations, making it a more expected calculation for drought events induced by rising temperatures. SPEI computation is similar to SPI computation (Getahun et al. 2023, Liu et al., 2021). The Penman–Monteith technique is commonly used to calculate reference evapotranspiration (ET), which is the quantity of water that evaporates and transpires under ideal conditions. Generally, a log-logistic distribution is exhibited for the SPEI at different time scales, as determined by the Kolmogorov–Smirnov test. The water balance is computed at each time step (monthly, seasonal, or yearly) by subtracting precipitation (P) from potential evapotranspiration (PET). The PET was calculated via the Penman–Monteith technique, which considers climatic factors such as the maximum-minimum temperature, wind speed, dew point, solar radiation, latitudinal position, and average height of the region of interest (Vicente--Serrano et al. 2010). The data were derived from Giovanni as daily data at the Nasa site (https://giovanni.gsfc.nasa.gov/giovanni/). The Penman–Monteith equation was applied to calculate the PET. The Penman–Monteith formula is as follows:

$$PET = \frac{0.408 \times \Delta \times (R_n - G) + \gamma \times \frac{900}{T+273} \times u \times (e_s - e_a)}{\Delta + \gamma \times (1 + 0.34 \times u)} \qquad (3)$$

where PET = potential evapotranspiration (in units of water depth, such as millimeters or inches per time period, often daily or monthly); Δ = slope of the vapor pressure curve (kPa/°C); R_n = net adiation at the crop surface (MJ/m^2/day); G = soil heat flux density (MJ/m^2/day); γ = psychometric constant (kPa/°C); T = mean daily air temperature (°C); u= wind speed at 2 meters above the surface (m/s); e_s = saturation vapor pressure (kPa); e_a = actual vapor pressure (kPa).

This algorithm was run for 21 years for three separate months, including premonsoon, monsoon, and postmonsoon data.

$$D_i = P - PET \qquad (4)$$

The quantity of water that might evaporate and transpire from the land surface under given climatic circumstances is referred to as potential evapotranspiration. The estimated water balance numbers are standardized so that they may be compared across geographies and time periods. On the basis of these data, the water balance values are fitted to a probability distribution (typically a normal or gamma distribution).

$$F(x) = \left[1 + \left(\frac{1}{x-y}\right)\right] \qquad (5)$$

2.5. Mann–Kendall test with Sen's slope estimator value

The Mann–Kendall (MK) test, a nonparametric test, was utilized in R-studio for trend analysis of seasonal and annual rainfall and temperature (Getahun et al. 2021). The Mann–Kendall test (Kendall., 1975) is a statistical technique used to identify trends in time series data. It is particularly valuable when dealing with data that do not follow a normal distribution or when outliers are present. The WMO recommends the use of this nonparametric test in climatic studies. This technique is extensively used to determine when a weather variable fluctuates substantially. In these test statistics, the null and alternative hypotheses are primarily considered. The Mann–Kendall test was applied to the SPI and SPEI results of different time scales. The Mann–Kendall statistic (S) is calculated by comparing the number of pairs of data points that exhibit a rising, decreasing or no trend.

$$S = \sum_{k=1}^{n-1} \sum_{j=k+1}^{n} sgn(x_j - x_k) \qquad (6)$$

where xi and xj are the ranking data values at periods i and j, respectively, and the sum of all unique pairs (i, j) with j > i is taken.

The variance of the Mann–Kendall statistic is calculated to determine the significance.

$$Var(S) = \frac{n(n-1)(2n+5)\sum_{i=1}^{m} t_1(i)(i-1)(2i+5)}{18} \qquad (7)$$

The Mann–Kendall statistic (S) is divided by the square root of the variance (Var(S)) to obtain the test statistic (Z).

$$Z = \left(S/\sqrt{Var\ (S)}\right) \qquad (8)$$

Sen's slope is a nonparametric approach for estimating the slope or trend in time series data. It is known as Sen's estimator (Sen., 1968). It is frequently used to analyze patterns in time series data in hydrology, climatology, environmental science, and other domains. It calculates each pairwise (i, j) difference between the data points.

$$Diff\ (i,j) = \left(X_j - X_i\right) \div (j - i) \qquad (9)$$

where xi and xj represent data values at periods i and j, respectively.

In this analysis, the Mann-Kendall test was employed to detect trends, with statistical significance established at a p-value threshold of 0.05.

2.6. Analysis of Drought and Future Predictions with the Holt-Winters Test

Holt-Winters smoothing is a time series forecasting approach that makes forecasts about future values via past data (Mishra & Desai, 2005). This method evaluates the trend, seasonality and level components from historical data and uses them to project future values beyond the given data. Trends and seasonality show a degree of continuity in climate indices such as the SPI and SPEI. As a result, the approach may yield relatively accurate forecasts for short- to medium-term time frames. In this study, a ten-year forecast was developed to demarcate the short-term future drought tendency in a realistic manner and enforce prompt action over the region. The key issue in predicting a random variable is determining the function of the probability density of future values on the basis of prior observations. The steps of this test are described below.

$$L_t = a(Y_t - S_{t-m}) + (1 - a)(L_{t-1} + b_{t-1}) \qquad (10)$$

$$b_t = \beta(T_t - L_{t-1}) + (1 - \beta)b_{t-1} \qquad (11)$$

$$S_t = y(Y_t - L_t) + (1 - \gamma)S_{t-m} \qquad (12)$$

$$F_{t+h} = L_{t+h}(T_t + S_{t+h-m}) \qquad (13)$$

Here, L_t, b_t, and S_t represent the observed value, level (baseline), and seasonal component at time t, respectively; α, β and γ are the smoothening parameters; h represents the periods of future prediction; and F_{t+h} represents the forecast of t+h.

The Holt-Winter forecasting method uses smoothing constants to adapt to time series data that exhibit trends and seasonal patterns. Alpha (α) adjusts the weight given to recent data when determining the series' average level. Beta (β) controls how much influence recent changes have on the estimated trend (the series' rate of increase or decrease). Gamma (γ) manages the weight given to recent seasonal factors within the recurring patterns of the series. By tuning these constants, the method balances the forecast's responsiveness to recent changes against its overall smoothness (Encik, 2015)

2.7. Trend of the groundwater level

The mean was computed via groundwater level data from all the borehole points in the Purulia district. From 1998–2018, three distinct mean values were determined. Three mean values were calculated on the basis of monsoonal, premonsoonal and postmonsoonal data. The R-square values were then assigned to each regression model to demonstrate how closely the regression line approximates the actual data.

3. Results

In this study, different types of calculations were performed to determine the frequency, intensity and magnitude of drought in this region over 21 years, and forecasts for the next 10 years were projected. This would help a suitable operation beforehand in the upcoming years.

3.1. Drought frequency

Drought frequency and severity have been evaluated through various statistical drought analyses. According to the requirements, the SPI and SPEI can be measured at various time scales. Here, 4, 6 and 12 monthly SPI and SPEI values were calculated. Purulia district is located under monsoonal climatic conditions. Therefore, 4 monthly SPIs and SPEs were needed to distinguish premonsoonal, monsoonal and postmonsoonal calculations. SPI-6 and SPEI-12 were required for semiannual drought assessment, and for annual drought, SPI-12 and SPEI-12 were highly applicable. There is a scale by McKee that demonstrates various drought categories according to values such as moderate, severe and extreme.

3.1.1. Results of SPI

A total of 252 months were considered for the calculation of the SPI. A total of 170, 24, 7 and 7 months were recognized as normal, moderate, severe and extreme drought months, respectively, by SPI-4. A total of 173, 19, 8 and 6 months of normal, moderate, severe and extreme drought months, respectively, were identified by the SPI-6. According to the SPI-12, 169 were normal, 25 were moderate drought months, and 10 were severe drought months within the period 1998-2018. The months in which the different SPI-based droughts are most prevalent are listed here.

Table 2 Occurrence of drought severity using the SPI at different times from 1998–2018.

SPI Time Scale	Drought Severity	Months
SPI-4	Extreme (7)	1999- Mar, Apr/2009-Feb/2010-Aug/2015-Nov, Dec/2017- Feb
	Severe (7)	2000-Oct/2009-Apr/2010-Jul, Sept, Oct/2012- May/2018-March
	Moderate (24)	1998-Jul, Aug/1999-May/2000-Sep, Nov/2001-Nov, Dec/2002-May/2004-May/2005-May-Sep/2006-Feb/2007- Jan/2008-Dec/2009-Jan/2010-Jun, Nov/2012-Jun/2016-Jan/2017-Jan
SPI-6	Extreme (6)	1999-May/2009- Apr/2010- Aug, Nov/2016- Jan, Feb
	Severe (8)	2000-Dec/2005- Sept/2009- Feb, Mar/2010- Jul, Sept, Oct, Dec
	Moderate (19)	1999-Apr/2000-Aug, Oct, Nov/2001-Jan/2002- Jan, Feb/2005- May-Nov/2009- Jan, Jun/2010- May, Jun/2016- Mar/2017- Mar
SPI-12	Extreme (0)	
	Severe (10)	2008- Aug, Sep/2010- Aug, Oct/2011- Jan-May/2016- Jul
	Moderate (25)	2000- Oct, Nov, Dec/2001-Jan-May/2002- Jul, Aug/2003- Jun, Sep/2005- Jun, Oct-Dec/2006- Jan-May/2009- Jun-Aug/2010-Aug

3.1.2. Results of the SPEI

SPEI has been run on this time period of 1998-2018. Here, 166, 23,14 and 3 months have been identified as normal, moderate, severe and extreme drought months by SPEI-4. Again, by SPEI-6, 22, 14, 3 and 170 were moderate, severe, extreme and normal drought months. Total 17, 8 and 5 months have been identified as moderate, severe and extreme drought months by SPEI-12. The months in which the different SPEI-based droughts are most prevalent are listed here.

3.2. Identification of Drought Trends

Trends in rainfall, temperature and PET throughout the eastern part of the Chotonagpur Plateau region were evaluated via the Mann–Kendall (M-K) test and Sen's slope test. To portray the trends in spatiotemporal drought characteristics, the M-K test was applied to SPI-4, SPI-6, and SPI-12 and to SPEI-4, 6, and 12. To consider the situations of the premonsoonal, monsoonal and postmonsoonal months, the test was applied to the SPI and SPEI values for May, September and January. The values of the SPI and SPEI revealed that most of the drought events were present in the premonsoonal period. However, the M-K test did not reveal any such prominent trend in this climatic data analysis. However, according to the results, Sen's estimator revealed a negative magnitude of dry months in the postmonsoonal period, whereas in the monsoonal and postmonsoonal periods, there was no such trend. In terms of Sen's slope, the magnitude decreased at the 5% level of significance to negative values in the postmonsoonal (January) SPI and SPEI analyses, such as -0.0193, -0.0163, and -0.0134 for the SPEI-4, SPEI-6 and SPI-4, respectively. If only postmonsoonal rainfall and evapotranspiration are considered, then the drought seasons are relatively more common. However, in the monsoonal and premonsoonal seasons, a slight positive magnitude was detected in the rest of the SPIs and SPEIs. For SPI-4, the magnitudes were 0.039 and 0.051 in May and September, respectively. For SPI-6, the magnitudes were 0.043, 0.064 and 0.057 in Jan, May and September, respectively. For SPI-12, 0.015, 0.0370, and 0.0474 were the magnitudes for January, May and September, respectively. In the case of the SPEI-4, the magnitude in May was 0.039, that in September was 0.051, and the estimated slope values were 0.051 and 0.034 in May and September, respectively. The slope values were 0.015, 0.037 and 0.048 in Jan, May, and September, respectively, for the SPEI-12.

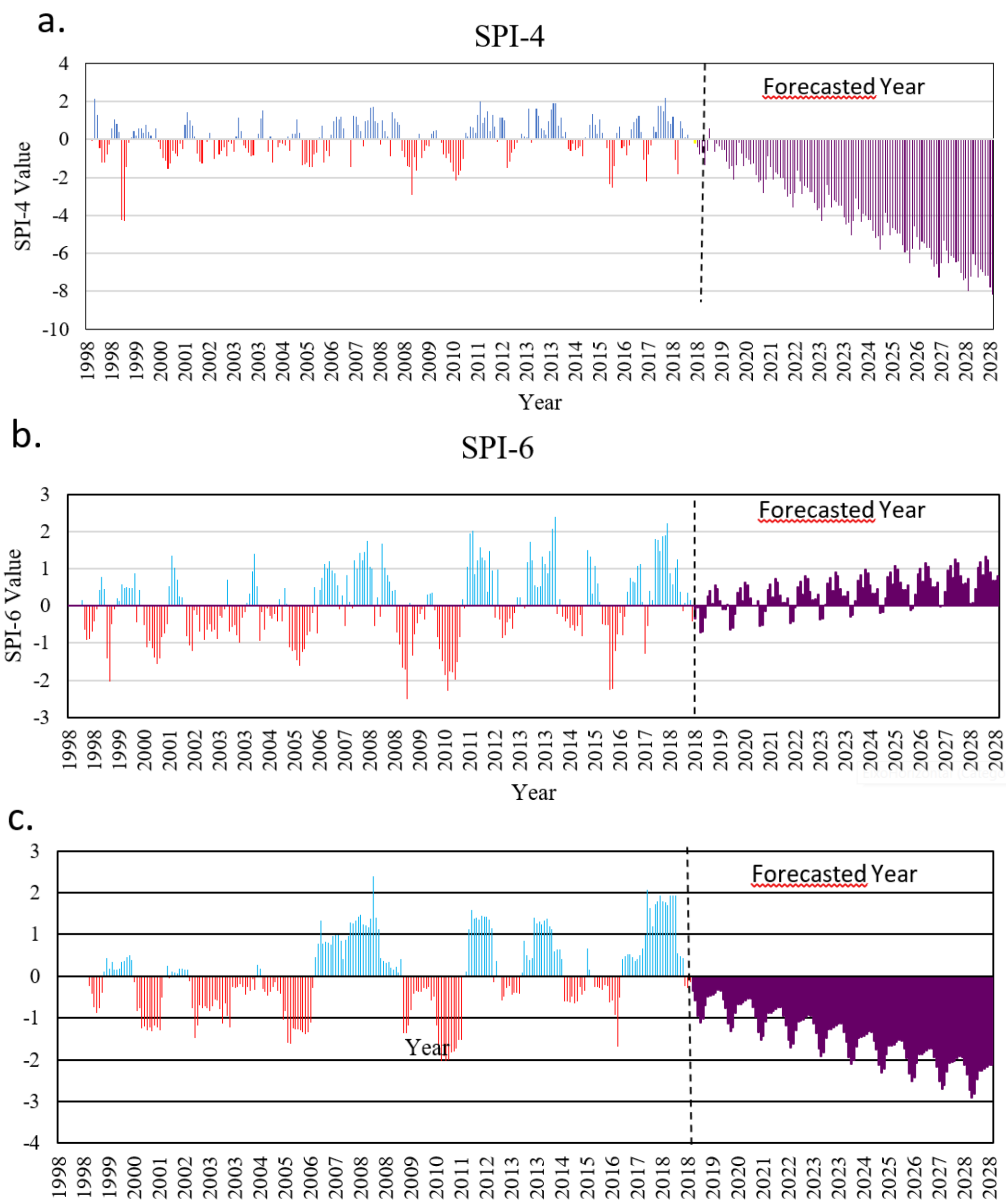

Figure 2 SPI for drought severity assessment, 1998-2028, a. 4-month time scale, b. 6-month time scale, c. 12-month time scale.

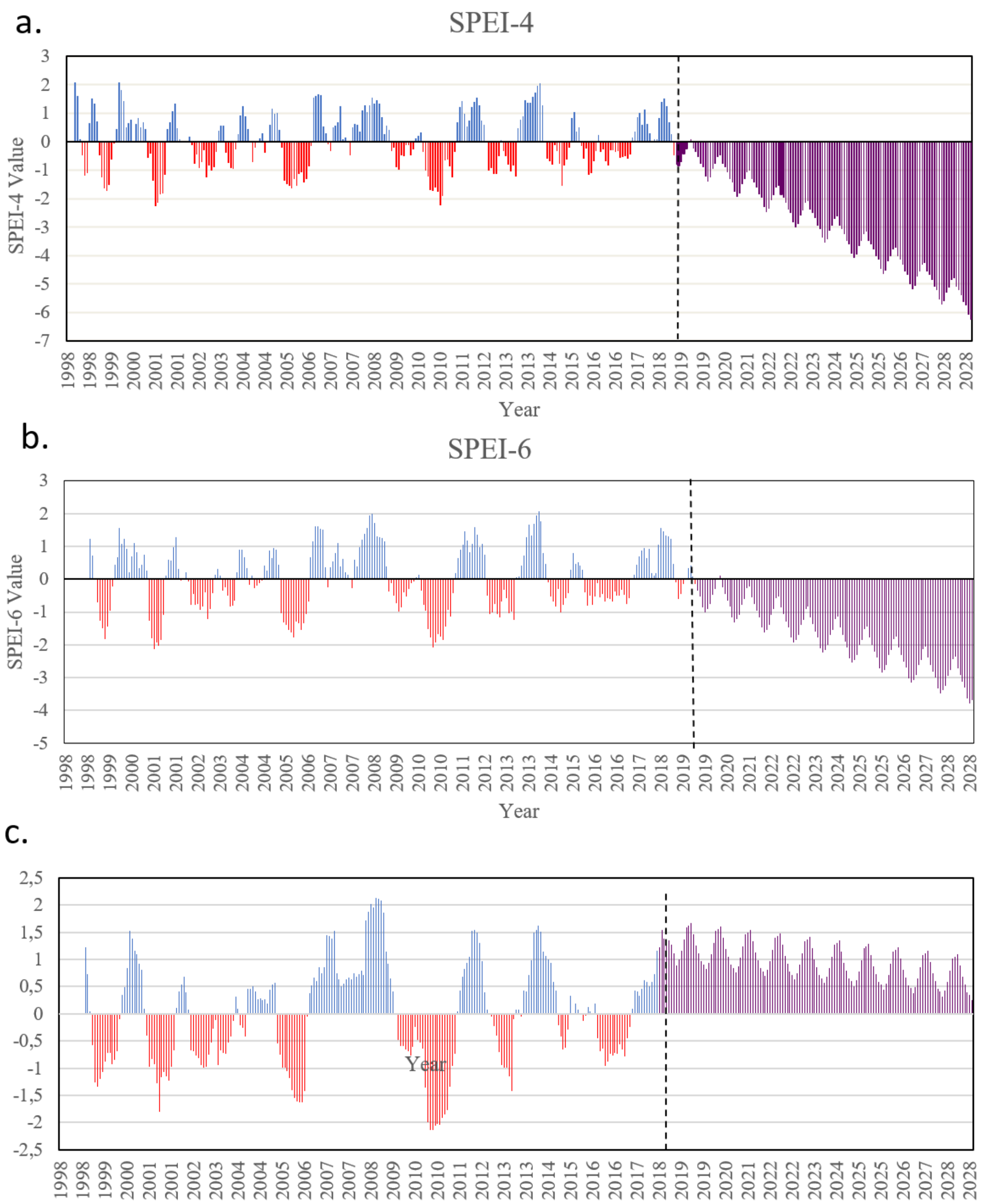

Figure 3 SPEI for drought severity assessment,1998-2028, a. 4-month time scale, b. 6-month time scale, c. 12-month time scale.

Table 3 Occurrence of drought severity via the SPEI at different times from 1998–2018.

SPEI Time Scale	Drought Severity	Months
SPEI-4	Extreme (3)	2001-Jan, Feb/2010-Oct
	Severe (14)	1999-Apr, May, Jun/2001-Mar, Apr/2005-Aug, Sept, Nov/2010-Jun-Nov/2014-Dec
	Moderate (23)	1998-Aug, Sept/1999-Mar/2000-Dec/2001- May/2002-Oct, Dec/2005-Jun, Oct, Dec/2006- Jan, Feb, Mar/2010- Apr, May/2011-Mar/2012-Jun, Aug, Sept/2013- Mar, May, Nov, Dec
SPEI-6	Extreme (3)	2001- Feb, Apr/2010-Aug
	Severe (14)	1999-Jun/2001- Jan, Mar, May/2005- Sept, Oct, Nov/2006- Feb/2010- Jun, Jul, Sept-Dec
	Moderate (22)	1999-Apr, May, Jul, Dec/2001- Jun/2002-Dec/2005- Jun-Aug, Dec/2006- Jan, Mar, Apr/2011- Jan, Mar/2012- July, Aug, Oct, Nov/2013- Mar, May/2014-Dec
EI-12	Extreme (5)	2010- Aug-Nov
	Severe (8)	2001-Aug/2006-Jan-Apr/2011-Jan-Mar
	Moderate (17)	1999-Apr-Jul/2001- May, Jul-Oct/2005-Oct-Nov/2006-May/2010-Jun/2011-Apr/2013-Apr, May

Table 4 MK test and Sen's slope analysis of the SPIs and SPEIs.

Index	Month	Z Score	P value	Kendall's tau	Sen's Slope
SPI4	All	2.279	0.023	0.096	0.002
	Jan	-0.151	0.88	-0.029	-0.013
	May	0.936	0.349	0.150	0.039
	Sept	1.419	0.156	0.230	0.051
SPI6	All	3.5	0	0.230	0.051
	Jan	0.936	0.349	0.150	0.043
	May	1.359	0.174	0.220	0.064
	Sept	1.54	0.124	0.250	0.057
SPI12	All	4.48	0	0.190	0.004
	Jan	0.936	0.349	0.150	0.039
	May	1.299	0.194	0.210	0.053
	Sept	1.48	0.139	0.240	0.03
SPEI4	All	0.37	0.711	0.016	0
	Jan	-0.211	0.833	-0.038	-0.019
	May	0.876	0.381	0.140	0.033
	Sept	0.151	0.88	0.029	0.007
SPEI6	All	1.296	0.195	0.055	0.001
	Jan	-0.332	8	-0.057	-0.016
	May	1.6	0.11	0.260	0.051
	Sept	0.876	0.381	0.140	0.034
SPEI12	All	3.15	0.002	0.130	0.003
	Jan	0.393	0.695	0.067	0.015
	May	0.574	0.566	0.095	0.037
	Sept	1.117	0.264	0.180	0.047

Table 5 Descriptive Statistics of the SPIs and SPEIs.

Informational Coefficient	SPI4	SPI6	SPI12	SPEI4	SPEI6	SPEI12
Minimum	-2.273	-2.521	-2.030	-4.312	-2.134	-2.145
Maximum	2.096	2.401	2.384	2.194	2.055	2.133
Mean	-0.001	0.007	0.005	-0.007	-0.002	0.000
Median	-0.016	-0.031	-0.011	0.045	-0.004	0.009
Variance	0.927	0.902	0.868	1.042	0.906	0.897
SD	0.963	0.950	0.932	1.021	0.952	0.947
Skewness	-0.007	0.008	0.119	-0.650	-0.053	-0.008
Kurtosis	-0.701	-0.285	-0.471	1.445	-0.691	-0.563

3.3. Holt-Winter Test and Forecasting

The Holt Winter algorithm is a time series forecasting approach that makes forecasts on the basis of prior data via exponential smoothing. A complete 10-year (January 2019--December 2028 total of 120 months) forecast was performed on the basis of the SPI and SPEI time series values. Three parameters, Alpha (α), Beta (β), and Gamma (γ), represent the level, trend and seasonality smoothing factors, respectively, which makes it more acceptable, as it considers many factors to calculate future predictions.

In the cases of SPI-4 and SPEI-4, there were more extreme drought situations, which means that only the seasonal rainfall was normal. As this region is under the monsoonal belt, it can be claimed that only monsoonal rainfall is normal here; otherwise, the region faces drought with high temperatures throughout the years. The SPEI-6 revealed that 20, 17 and 43 months represented moderate, severe and extreme drought, respectively, but according to the SPI-6, there was no drought month. For SPI-12, 29, 31 and 29 were extreme, severe and moderate drought months, respectively, and there was no single year of drought in SPI-6 and SPEI-12. It can be concluded that in the following year, most drought events will occur due to high temperatures. Rainfall variability and the duration of rainfall may differ, which can lead to seasonal drought. If rainfall occurs at an unusual time compared with normal, it might alleviate drought conditions in those months but could worsen drought conditions during the typical rainy months, thereby creating adverse conditions for the sociocultural life of human beings.

Insufficient rainfall is present, which may result in a lower drought count, but it adversely affects the sociocultural life of the local population. Overall, this situation indicates a decreasing trend in rainfall.

3.4. Correlation between the SPI and SPEI analysis

Pearson's correlation is used to classify the degree of relationship between the SPI and SPEI at various time scales. Where the SPI considers historical precipitation data, the SPEI uses potential evapotranspiration along with precipitation, and these two values are also calculated on the basis of standardization, the Pearson correlation is perfect in this study. Here, the strongest positive relationship was observed between the SPI12 and SPEI12, followed by between the SPI6 and SPEI6 and between the SPI4 and SPEI4. The lowest correlation was observed between SPI6 and SPEI12, followed by SPI12 and SPEI4 and between SPI4 and SPEI12.

Table 6 Drought intensity according to Holt-Winter tests from 2019–28.

Index	Drought intensity		
	Moderate	Severe	Extreme
SPI-4	9	5	>25
SPI-6	-	-	-
SPI-12	>25	>25	>25
SPEI-4	11	12	19
SPEI-6	20	17	>25
SPEI-12	-	-	-

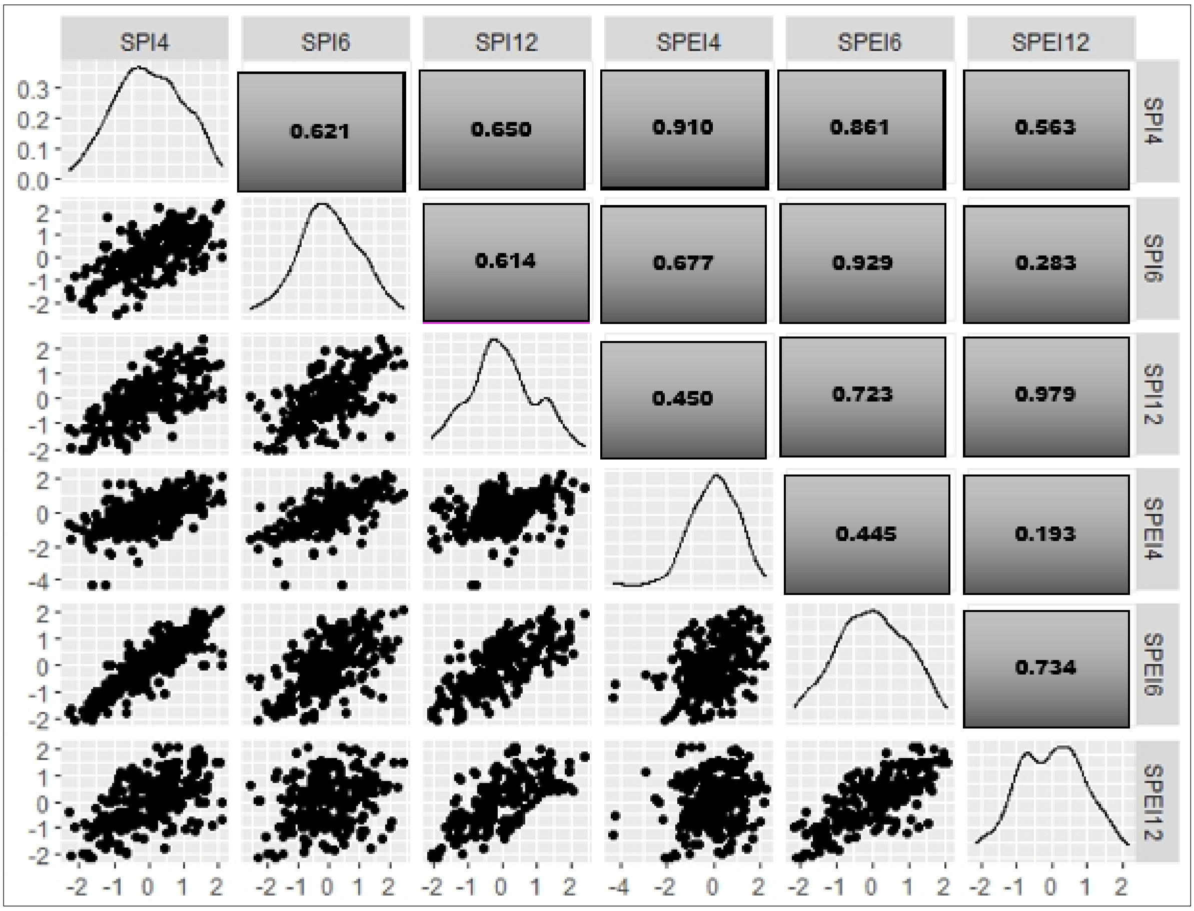

Figure 4 Correlation matrix, correlation between SPI & SPEI in different time scale.

Table 7 Smoothing Parameters of the Holt-Winter Test.

Smoothing Parameter	SPI-4	SPI-6	SPI-12	SPEI-4	SPEI-6	SPEI-12
Alpha	0.602	0.713	1.000	0.701	0.748	0.760
Beta	0.000	0.000	0.000	0.001	0.004	0.007
Gamma	0.875	0.893	1.000	1.000	1.000	1.000
RMSE	1.132	0.786	0.435	0.739	0.599	0.482
MAE	0.823	0.564	0.308	0.576	0.465	0.337
MPE	106.681	366.440	112.152	118.474	50.232	-7.833
MAPE	344.477	686.365	178.794	297.760	150.513	157.598
MASE	0.669	0.482	0.274	0.447	0.360	0.268

3.5. Trend of Groundwater Level

Groundwater level data were downloaded and examined with mean values of premonsoonal, monsoonal, and postmonsoonal data.

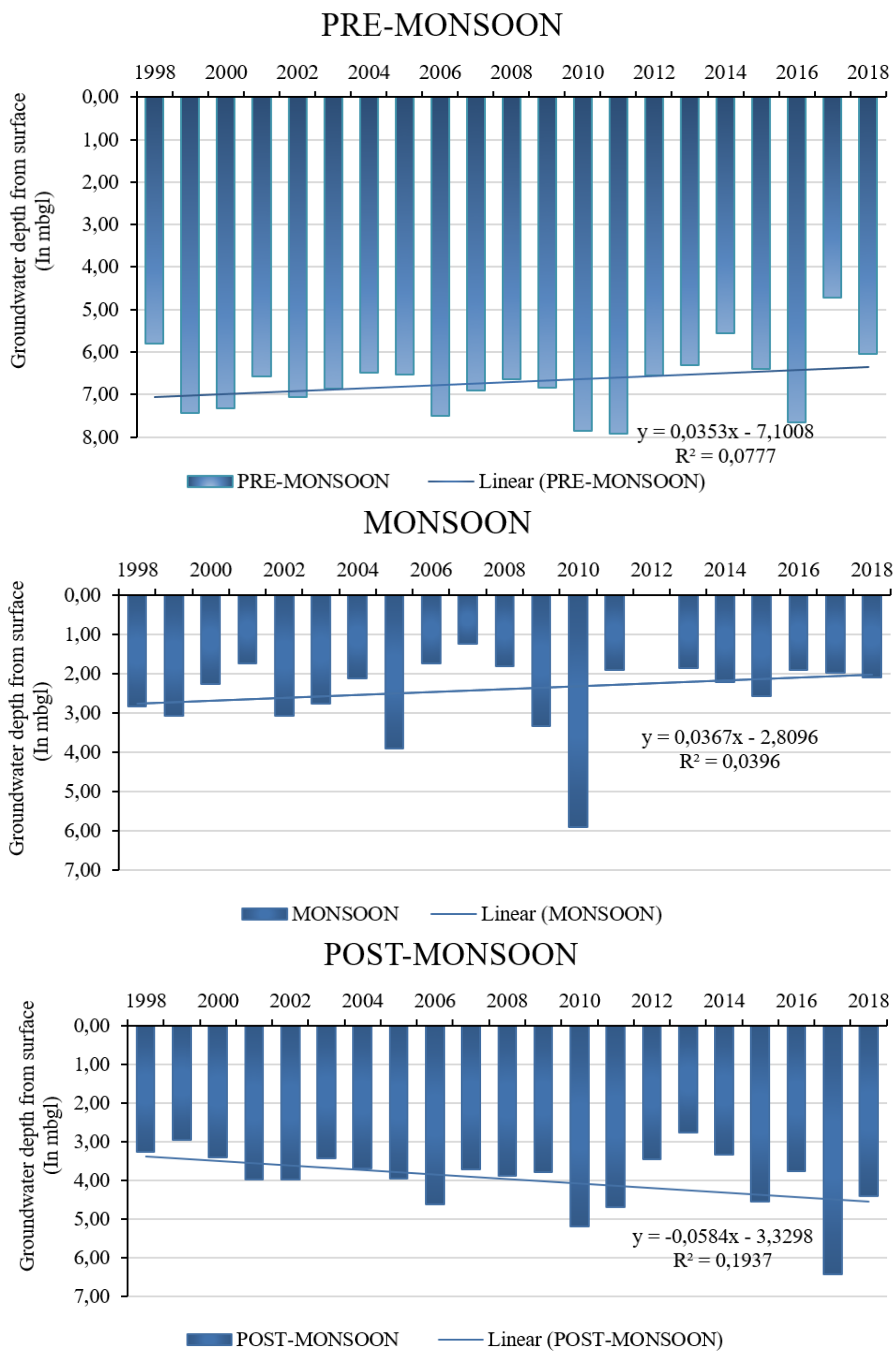

Figure 5 Groundwater Depth from Surface of Pre-Monsoon, Monsoon and Post-Monsoon period.

A premonsoon study revealed that the average depth was greater than 6 mbgl (m below ground level) over the years, although the level increased daily. During the monsoon season, the average gap between the water level and the surface was greater than 2 mbgl, and the trend line exhibited a negative trend, indicating an increasing trend in the water level. The postmonsoonal research produced a unique finding in which the average depth in these 21 years was 4 m, with a declining rate of water level. The water level increased throughout the premonsoonal and monsoonal periods, indicating a large supply of water. Conversely, the water level decreased during the postmonsoon period, indicating a poor recharge rate.

4. Discussion

This study was carried out to demonstrate meteorological drought, with specific reference to the SPI and SPEI, as well as its trend. In addition, the Holt-Winters test was carried out to forecast the coming ten years beginning in 2018. A meteorological drought study revealed that 1999, 2005, 2009, 2010 and 2016 were the month's most prone to drought between 1998 and 2018. The results are closely aligned with previous studies. Bera et al. (2021) found that the moderate and mild drought years were in various months of 2000, 2004, 2005, 2010, 2016 and extreme drought were in 1999, 2001, 2003, 2014, 2015 and 2016. Similarly, Bhunia et al. (2019) stated that the months of 2003, 2014 and 2016 as Moderate Drought, 1998, 2000 and 2002 as severe drought and 2000, 2015 and 2016 was extreme drought period.

Except for any specific meteorological year (El-Nino-1997-98, 2002-03, 2006-07, 2009-10, 2015-16, 2018-19 and La-Nina-1998-01, 2007-09, 2008-09, 2010-12, by NOAA), the periodic SPI (SPI4) indicated that extreme or severe drought occurred primarily between January and April. Chales Todd (1888) suggested that the effects of El Nino and La Nina hit Australia and India at the same time. In 2009, 14 states declared drought, a drought-like situation, or a shortage in 338 districts of the nation because of insufficient and unpredictable rainfall from the southwestern monsoon. The failure of India's monsoon, which increased food costs, and the 2009–10 El Nino weather pattern worsened India's drought. Approximately 2,000 people were killed by a severe El Nino in 1998, which also destroyed agriculture, infrastructure and mining in Australia and Asia for billions of Euros. Extreme occurrences such as droughts in Brazil and the Philippines and high temperatures in India and Thailand are just two examples of how the 2015–16 El Nino phenomenon has affected the world's climate. Over 2,000 people have died in the southern and eastern regions of India due to heat waves that lasted for many weeks. In these years, El Niño events were most severe.

To determine the period of rainfall in this climatic region, a four-month standardization process is needed. This result indicated that there was no rain from November to May, resulting in severe weather conditions. The extreme drought months for SPI-6 and SPI-12 were from January to July owing to a lack of rainfall. The M-K test revealed that the overall trend of the May and September SPIs revealed no such negative or positive trend; however, the SPI-4 in January presented a negative tendency, which meant that postmonsoon rainfall decreased. Interestingly, substantially larger positive values of the May SPI indicated that premonsoonal precipitation increased slightly more than monsoonal rainfall did. According to the SPEI, the most severe drought incidents occurred from March to August and from October to December. Owing to very high temperatures in the summer months, which may reach 50°C, the SPEI indicates more drought months than SPIs do. The granitic gneissic and mica-schist area experiences very high evapotranspiration (Mitra and Acharya, 2015), and the majority of this district features a volcanic rock structure. Here, the bare granite formations and intense insolation assisted in evaporating more. The SPEI-4 and SPEI-6 in January revealed a negative trend, and the propensity for drought in this region increased under periodic or semiannual conditions. Again, SPEIs for May demonstrated greater positive values, indicating that premonsoonal drought month counts were lower than those of the monsoonal drought month. The key finding of this study is that droughts are anticipated to occur at an alarming rate during the postmonsoonal season, whereas the premonsoonal phase would receive considerably more rainfall.

Furthermore, the predictions for the next 10 years generated for all SPIs and SPEIs indicated a tendency toward decreasing precipitation rates throughout the year. The Holt-Winters test considers both seasonality and trends, despite the trend previously not indicating this much negative rainfall, which showed a diminishing rate of change in terms of seasonality and amount of change. There is a significant chance of receiving less rain, and drought may worsen from the current situation. According to Choudhury et al. (2021), the trend of drought during the monsoon season over the Gangetic and the Brahmaputra plain has increased significantly, along with low long-period average rainfall (Pai et al., 2011).

Drought is a recurring natural crisis, not an unforeseen natural disaster. Identifying and anticipating drought patterns in semiarid areas is an important tool for long-term water resource management planning. In this projection, SPI-4 or periodical rainfall would cause more drought during postmonsoon times, whereas SPEI-6 or semiannual climatic conditions (precipitation and evapotranspiration) would aid in the occurrence of drought instances.

This area experiences moderate to low precipitation during the monsoon months and heavy rainfall during the postmonsoon season, with approximately 80% of the precipitated water flowing as surface runoff due to the rolling landscape. Similarly, percolated water drains as subsurface runoff due to the presence of many first- and second-generation structural components, such as bedding planes, faults, folds, fractures, and foliation. Unscientific groundwater removal for agriculture has been practiced in recent years. As a result, the groundwater table is rapidly falling, accelerating hydrological and agricultural dryness in India's semiarid climatic zone. The changing trend of climatic character not only hindering the Ganga Delta region but also Mekong Delta in Vietnam primarily due to the irregular monsoonal rainfall (Sarkar et al., 2024).

5. Conclusions

The main problem in this region is water stress. Owing to its physiography, different types of droughts are observed throughout the district. Hence, it is essential to analyze drought types. Here, variability in monsoonal rainfall and drought conditions occurs immediately after the monsoon, highlighting that the timing of rainfall is not regular from July to September.

A tendency toward a high precipitation rate in the premonsoonal period also demands water management, and agricultural practices should be checked according to the availability of water and rainfall tendency. Natural factors such as climate, groundwater, and surface water availability should be monitored regularly. As climatic conditions are changing, management strategies should accordingly be changed. Extrees in rainfall and temperature pose a risk to agriculture, food security, and socioeconomic vulnerability. Groundwater level research and data are critical for the survival of marginal farmers and tribal groups. To investigate the synergetic impacts of trends and patterns in other climatic variables, a more extensive structural study is necessary. High-temperature-resistant plants and seeds should be grown, and farmers should be encouraged to grow these crops. The results of this study might constitute a first step toward improving the risk management approach, farming practices and water consumption in this region.

Ethical considerations

This study involved the analysis of bibliometric data and did not include any human or animal subjects. No individuals or communities were harmed or involved in the research process. All methods were conducted in accordance with ethical guidelines for academic research.

Conflict of Interest

The authors declare no conflicts of interest.

Funding

This research did not receive any financial support.

References

Ahmadalipour, A., Moradkhani, H., Castelletti, A., & Magliocca, N. (2019). Future drought risk in Africa: Integrating vulnerability, climate change, and population growth. *Science of the Total Environment, 662*, 672–686.

Ahmadi, S. H., & Sedghamiz, A. (2007). Geostatistical analysis of spatial and temporal variations of groundwater level. *Environmental Monitoring and Assessment, 129*, 277–294.

Barrios, M., Borrego, A., Vilaginés, A., Ollé, C., & Somoza, M. (2008, September 17). A bibliometric study of psychological research on tourism. *Scientometrics, 77*(3), 453–467. https://doi.org/10.1007/s11192-007-1952-0

Bera, B., Shit, P. K., Sengupta, N., Saha, S., & Bhattacharjee, S. (2021). Trends and variability of drought in the extended part of Chhota Nagpur Plateau (Singbhum Protocontinent), India applying SPI and SPEI indices. *Environmental Challenges, 5*, 100310.

Bhalme, H. N., & Mooley, D. A. (1980). Large-scale droughts/floods and monsoon circulation. *[Journal Name]*. *(Note: Add journal name and volume if available).*

Bhunia, P., Das, P., & Maiti, R. (2019). Meteorological drought study through SPI in three drought prone districts of West Bengal, India. *Earth Systems and Environment, 4*(1), 43–55. https://doi.org/10.1007/s41748-019-00137-6 *(Duplicate of 2020 reference; keep only one)*

Byun, H. R., & Wilhite, D. A. (1999). Objective quantification of drought severity and duration. *Journal of Climate, 12*(9), 2747–2756.

Choudhury, A., Dutta, D., Bera, D., & Kundu, A. (2021). Regional variation of drought parameters and long-term trends over India using standardized precipitation evapotranspiration index. *Journal of Environmental Management, 296*, 113056.

Ding, Y., Gong, X., Xing, Z., Cai, H., Zhou, Z., Zhang, D., ... & Shi, H. (2021). Attribution of meteorological, hydrological and agricultural drought propagation in different climatic regions of China. *Agricultural Water Management, 255*, 106996.

District Disaster Management Plan 2021–2022, Purulia. Office of the District Magistrate, Purulia Disaster Management Section.

Encik, R. (2015). Holt-Winter forecasting method to predict the number of visitors to the Riau University library. *Universitas Riau*.

Getahun, Y. S., & Li, M. H. (2023). Flash drought evaluation using evaporative stress and evaporative demand drought indices: A case study from Awash River Basin (ARB), Ethiopia. *Theoretical and Applied Climatology*, 1–20.

Getahun, Y. S., Li, M. H., & Pun, I. F. (2021). Trend and change-point detection analyses of rainfall and temperature over the Awash River Basin of Ethiopia. *Heliyon, 7*(9).

Getahun, Y. S., Li, M. H., Chen, Y. Y., & Yate, T. A. (2023). Drought characterization and severity analysis using GRACE-TWS and MODIS datasets: A case study from the Awash River Basin (ARB), Ethiopia. *Journal of Water and Climate Change, 14*(2), 516–542.

Ground Water Yearbook of West Bengal & Andaman & Nicobar Islands (2021–2022). Central Ground Water Board, Government of India.

Heim Jr, R. R. (2002). A review of twentieth-century drought indices used in the United States. *Bulletin of the American Meteorological Society, 83*(8), 1149–1166.

Jha, S., Sehgal, V. K., Raghava, R., & Sinha, M. (2013). Trend of standardized precipitation index during Indian summer monsoon season in agroclimatic zones of India. *Earth System Dynamics Discussions, 4*(1), 429–449.

Kendall, M. G. (1975). *Rank correlation methods* (4th ed.). Charles Griffin.

Kotchoni, D. V., Vouillamoz, J. M., Lawson, F. M., Adjomayi, P., Boukari, M., & Taylor, R. G. (2018). Relationships between rainfall and groundwater recharge in seasonally humid Benin: A comparative analysis of long-term hydrographs in sedimentary and crystalline aquifers. *Hydrogeology Journal*.

Kumar, K. N., Rajeevan, M., Pai, D. S., Srivastava, A. K., & Preethi, B. (2013). On the observed variability of monsoon droughts over India. *Weather and Climate Extremes, 1*, 42–50.

Kundu, A., Patel, N. R., Denis, D. M., & Dutta, D. (2020). An estimation of hydrometeorological drought stress over the central part of India using geo-information technology. *Journal of the Indian Society of Remote Sensing, 48*, 1–9.

Ledger, M. E., Edwards, F. K., Brown, L. E., Milner, A. M., & Woodward, G. (2011). Impact of simulated drought on ecosystem biomass production: An experimental test in stream mesocosms. *Global Change Biology, 17*(7), 2288–2297.

Li, L., She, D., Zheng, H., Lin, P., & Yang, Z. L. (2020). Elucidating diverse drought characteristics from two meteorological drought indices (SPI and SPEI) in China. *Journal of Hydrometeorology, 21*(7), 1513–1530.

Liu, Q., Zhang, S., Zhang, H., Bai, Y., & Zhang, J. (2020). Monitoring drought using composite drought indices based on remote sensing. *Science of the Total Environment, 711*, 134585.

McGuire, J. K., & Palmer, W. C. (1957). The 1957 drought in the eastern United States. *Monthly Weather Review, 85*, 305–315.

McKee, T. B., Doesken, N. J., & Kleist, J. (1995). Drought monitoring with multiple time scales. In *Proceedings of the Ninth Conference on Applied Climatology* (pp. 233–236). American Meteorological Society.

Meyer, S. J., Hubbard, K. G., & Wilhite, D. A. (1993). A crop-specific drought index for corn: I. Model development and validation. *Agronomy Journal, 85*(2), 388–395.

Mishra, A. K., & Desai, V. R. (2005). Drought forecasting using stochastic models. *Stochastic Environmental Research and Risk Assessment, 19*, 326–339.

Mitra, M., & Acharya, T. (2015). Study of fractures in Precambrian crystalline rocks using field technique in and around Balarampur, Purulia district, West Bengal, India. *Journal of Earth System Science, 124*, 1801–1812.

Narasimhan, B., & Srinivasan, R. (2005). Development and evaluation of Soil Moisture Deficit Index (SMDI) and Evapotranspiration Deficit Index (ETDI) for agricultural drought monitoring. *Agricultural and Forest Meteorology, 133*(1–4), 69–88.

Pai, D. S., Sridhar, L., Guhathakurta, P., & Hatwar, H. R. (2011). District-wide drought climatology of the southwest monsoon season over India based on standardized precipitation index (SPI). *Natural Hazards, 59*(3), 1797–1813. https://doi.org/10.1007/s11069-011-9867-8

Palmer, W. C. (1968). Keeping track of crop moisture conditions, nationwide: The new crop moisture index.

Palmer, W. C. (1965). *Meteorological drought* (Research Paper No. 45). Weather Bureau.

Panday, S. C., Kumar, A., Meena, V. S., Joshi, K., Stanley, J., & Pattanayak, A. (2020). Standardized precipitation index (SPI) for drought severity assessment of Almora, Uttarakhand, India. *Journal of Agrometeorology, 22*(2), 203–206.

Parthasarathy, B., Sontakke, N. A., Monot, A. A., & Kothawale, D. R. (1987). Droughts/floods in the summer monsoon season over different meteorological subdivisions of India for the period 1871–1984. *Journal of Climatology, 7*(1), 57–70.

Pathak, A. A., & Dodamani, B. M. (2019). Trend analysis of groundwater levels and assessment of regional groundwater drought: Ghataprabha River Basin, India. *Natural Resources Research, 28*, 631–643.

Poornima, S., & Pushpalatha, M. (2019). Drought prediction based on SPI and SPEI with varying timescales using LSTM recurrent neural network. *Soft Computing, 23*, 8399–8412.

Raha, S., & Gayen, S. K. (2019). Simulation of meteorological drought of Bankura District, West Bengal: Comparative study between exponential smoothing and machine learning procedures. *Journal of Geography, Environment and Earth Science International, 22*(1), 1–16.

Rehana, S., & Monish, N. T. (2020). Characterization of regional drought over water and energy limited zones of India using potential and actual evapotranspiration. *Earth and Space Science, 7*(10), e2020EA001264.

Roy, P., Pal, S. C., Chakrabortty, R., Chowdhuri, I., Saha, A., & Shit, M. (2022). Climate change and groundwater overdraft impacts on agricultural drought in India: Vulnerability assessment, food security measures and policy recommendation. *Science of The Total Environment, 849*, 157850.

Roy, S., Hazra, S., & Chanda, A. (2023). Changing characteristics of meteorological drought and its impact on monsoon-rice production in sub-humid red and laterite zone of West Bengal, India. *Theoretical and Applied Climatology, 151*(3–4), 1419–1433.

Vicente-Serrano, S. M., López-Moreno, J. I., Beguería, S., Lorenzo-Lacruz, J., Azorin-Molina, C., & Morán-Tejeda, E. (2012). Accurate computation of a streamflow drought index. *Journal of Hydrologic Engineering, 17*, 318–332.

Sarkar, B., Mohinuddin, S., Islam, A., Islam, A. R. M. T., Saha, U. D., Sengupta, S., Pal, S. C., Chu, H., & Huang, J. (2024). SPI-gamma random forest modelling for meteorological drought characterization and prediction in the Bengal Delta, Indo-Bangladesh region. *Theoretical and Applied Climatology, 156*(1). https://doi.org/10.1007/s00704-024-05293-y

Sen, P. K. (1968). Estimates of the regression coefficient based on Kendall's tau. *Journal of the American Statistical Association, 63*(324), 1379–1389.

Shafer, B. A., & Dezman, L. E. (1982). Development of a Surface Water Supply Index (SWSI) to assess the severity of drought conditions in snowpack runoff areas. In *Proceedings of the Western Snow Conference* (pp. 164–175).

Shah, R., Bharadiya, N., & Manekar, V. (2015). Drought index computation using standardized precipitation index (SPI) method for Surat District, Gujarat. *Aquatic Procedia, 4*, 1243–1249.

Shukla, S., & Wood, A. W. (2008). Use of a standardized runoff index for characterizing hydrologic drought. *Geophysical Research Letters, 35*(2).

Shahfahad, Talukdar, S., Ghose, B., Islam, A. R. M. T., Hasanuzzaman, M., Ahmed, I. A., & Afzal, M. (2023). Predicting long term regional drought pattern in Northeast India using advanced statistical technique and wavelet-machine learning approach. *Modeling Earth Systems and Environment*, 1–22.

Shaik, D. S., Kant, Y., Mitra, D., Singh, A., Chandola, H. C., Sateesh, M., ... & Chauhan, P. (2019). Impact of biomass burning on regional aerosol optical properties: A case study over northern India. *Journal of Environmental Management, 244*, 328–343.

Singh, R. M., & Shukla, P. (2020). Drought characterization using drought indices and El Nino effects. *National Academy Science Letters, 43*, 339–342.

Todd, C. (1888). *The Australasian*, 1456.

Tsakiris, G. (2017). Drought risk assessment and management. *Water Resources Management, 31*, 3083–3095.

Tsakiris, G., & Vangelis, H. J. (2005). Establishing a drought index incorporating evapotranspiration. *European Water, 9*(10), 3–11.

Van Rooy, M. P. (1965). A rainfall anomaly index (RAI) independent of time and space. *Notos, 14*, 43–48.

Wang, J., Lin, H., Huang, J., Jiang, C., Xie, Y., & Zhou, M. (2019). Variations of drought tendency, frequency, and characteristics and their responses to climate change under CMIP5 RCP scenarios in Huai River Basin, China. *Water, 11*(10), 2174.

Zhai, J., Mondal, S. K., Fischer, T., Wang, Y., Su, B., Huang, J., ... & Uddin, M. J. (2020). Future drought characteristics through a multi-model ensemble from CMIP6 over South Asia. *Atmospheric Research, 246*, 105111.